

# A comparative study on 2D crack modelling using the extended finite element method

S.J. Rouzegar\*, M. Mirzaei\*\*

\*Shiraz University of Technology, Modares Boulevard, Shiraz 71555-313, Iran, E-mail:rouzegar@sutech.ac.ir

\*\*Tarbiat Modares University, Jalal Ale Ahmad Highway, Tehran 14115-111, Iran, E-mail: mmirzaei@modares.ac.ir

crossref <http://dx.doi.org/10.5755/j01.mech.19.4.5043>

## 1. Introduction

In general, the current crack modelling methods can be classified into two broad categories of geometrical and non-geometrical presentations. In the first category, the presence of a crack in the model is explicit and the geometry and mesh are changed during the crack growth [1, 2]. In the second category, the crack does not appear in the model as a physical object but its presence affects the governing equations. These effects are either on the stress-strain constitutive equations or on the strain-displacement kinematic equations. The latter approach is implemented in the Extended Finite Element Method (XFEM) by adding extra functions (enrichment functions) to the approximation space of the elements around the crack. This process gives additional degrees of freedom to the enriched nodes. This method, which was established based on the Partition of Unity Method (PUM) and applied to fracture mechanics problems by Belytschko and Black [3], was improved by Dolbow for crack growth modelling without re-meshing [4]. The method was later applied to other problems such as 3D fracture [5], dynamic problems [6], cohesive crack modelling [7], fracture mechanics of functionally graded materials (FGM) [8], and crack modelling in orthotropic materials [9]. A very recent review of the usage of the XFEM in computational fracture mechanics is reported in ref. [10].

Applications of the XFEM to plates and shells have been reported by Dolbow et al [11] for Mindlin-Reissner plates and by Areias et al [12, 13] for shells. Nevertheless, the focus of the current study is on the XFEM formulation based on the Kirchhoff plate theory [14], which is the simplest approach to the out-of-plane fracture problems. This approach can give accurate results for thin plates without the complications due to shear locking. In sequel a new set of Tip functions are extracted from analytical solutions of Kirchhoff plates [15, 16]. Accordingly, different enrichment schemes are implemented for constant strain triangle (CST) and quadrilateral (Q4) elements and the stress intensity factors (SIF) for several benchmark problems are calculated using the J-Integral and the Interaction Integral methods.

## 2. Basic formulations

The following sections present the basic aspects of the formulations and the enrichment schemes implemented in this study.

### 2.1. Plane XFEM formulation

Consider the domain  $\Omega \subset \mathfrak{R}^2$  bounded by  $\Gamma$  as shown in Fig. 1. The prescribed displacements and tractions are imposed on  $\Gamma_u$  and  $\Gamma_t$  respectively. The crack surface,  $\Gamma_d$  is assumed to be traction-free. The equilibrium equations and boundary conditions are:

$$\left. \begin{aligned} \nabla \boldsymbol{\sigma} + \mathbf{b} &= 0 & \text{in } \Omega; \\ \boldsymbol{\sigma} \mathbf{n} &= \bar{\mathbf{t}} & \text{on } \Gamma_t; \\ \boldsymbol{\sigma} \mathbf{n} &= 0 & \text{on } \Gamma_d, \end{aligned} \right\} \quad (1)$$

in which,  $\mathbf{n}$  is the outward unit normal,  $\boldsymbol{\sigma}$  is the Cauchy stress tensor, and  $\mathbf{b}$  is the body force density. In the classical finite element method, the solution space  $\mathbf{v}^h$  is constructed from low order polynomials  $\boldsymbol{\varphi}_i$  as:

$$\mathbf{v}^h \equiv \text{span} \{ \boldsymbol{\varphi}_i \}_{i=1}^N. \quad (2)$$

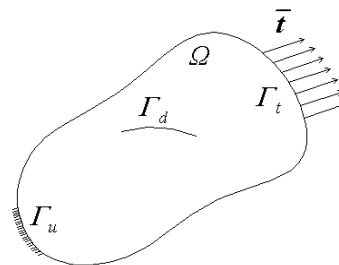


Fig. 1 A 2D domain with internal boundary subjected to external loads

However, in fracture mechanics problems where local behaviours (or rough solutions) exist, these polynomials usually do not give satisfying results unless either very fine meshes are used or the order of polynomials is increased. The aim of the XFEM is to avoid these difficulties by incorporation of simple analytical expressions into the solution space of the classical FEM. These expressions, obtained from the analytical solutions of a 2D elastic cracked domain under biaxial loading, are [3].

$$\left. \begin{aligned} \Psi_1 &= \sqrt{r} \sin(\theta/2); \\ \Psi_2 &= \sqrt{r} \cos(\theta/2); \\ \Psi_3 &= \sqrt{r} \sin(\theta) \sin(\theta/2); \\ \Psi_4 &= \sqrt{r} \sin(\theta) \cos(\theta/2), \end{aligned} \right\} \quad (3)$$

where  $r$  and  $\theta$  are the local polar coordinates at the crack tip. It should be noted that the first function is discontinu-

ous across the crack faces whereas the remaining functions are continuous. In 1999, Dolbow added the Heaviside discontinuous ( $H$ ) function to the above terms to also model the discontinuity along the crack wake. The  $H$  function is defined as [4]:

$$H(x) = \begin{cases} 1 & \text{for } (x-x^*)e_n > 0; \\ -1 & \text{for } (x-x^*)e_n < 0, \end{cases} \quad (4)$$

where  $x$  is a sample point,  $x^*$  (which lies on the crack) is the closest point projection of  $x$ , and  $e_n$  is the unit outward normal to the crack at  $x^*$ . In the XFEM terminology, the procedure of increasing the degrees of freedom of the nodes around the crack is called enrichment and is done locally, i.e., only selected nodes are enriched. The enriched displacement approximation can be written as:

$$u^h(x) = \sum_{i=1}^I N_i(x)u_i + \sum_{j=1}^J N_j(x)H(x)a_j + \sum_{k=1}^K N_k(x) \sum_{\alpha=1}^4 \Psi_\alpha(x)b_{\alpha k}, \quad (5)$$

where  $I$  is the set of all nodes,  $J$  is the set of nodes whose support is entirely split by the crack, and  $K$  is the set of nodes that contain the crack tip in their support. Also  $u_i$  are the nodal displacements,  $a_j$  and  $b_{\alpha k}$  are the degrees of freedom related to  $H$  and  $Tip$  functions.

## 2.2. Enrichment schemes for 2D problems

In a general enrichment procedure three distinct areas are distinguished, i.e., the area composed of elements all nodes of which are enriched ( $\Omega^{enr}$ ), the area where none of the nodes is enriched ( $\Omega^{std}$ ), and the area which only some of the nodes are enriched (called the blending area,  $\Omega^{blend}$ ). Since the blending elements are only ‘‘partially enriched’’, the enriched nodes in these elements do not form a partition of unity [17]. These elements play an important role in the approximation properties and must be handled with cautious. Accordingly, five types of elements are distinguishable as depicted in Fig. 2. The elements of type 1 form  $\Omega^{std}$ , the elements of type 2 and 3 form  $\Omega^{enr}$ , and the elements of type 4 and 5 form  $\Omega^{blend}$ . Because of the presence of the enrichment functions (especially the crack  $Tip$  functions) in the basis function of the approximation space, there are some deficiencies in the formulations of the elements of type 3 and elements of  $\Omega^{blend}$  (especially the elements of type 4).

There are also additional issues regarding the computation of energy on contours cutting these elements (these contours are often used for determination of the J-Integral or the Interaction Integral). Hence, it can be expected that if only the  $H$  function is used for the enrichment and the  $Tip$  functions are not considered, two problematic element types (type 3 and 4) will be omitted and the modelling procedure would be more efficient (see Fig. 3).

In sequel the effects of the elimination of the  $Tip$  functions from the enrichment scheme will be studied in more detail.

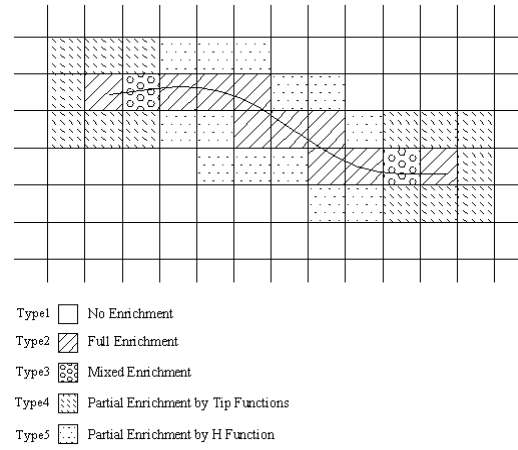


Fig. 2 Different areas of enrichment by both the  $H$  and the  $Tip$  functions

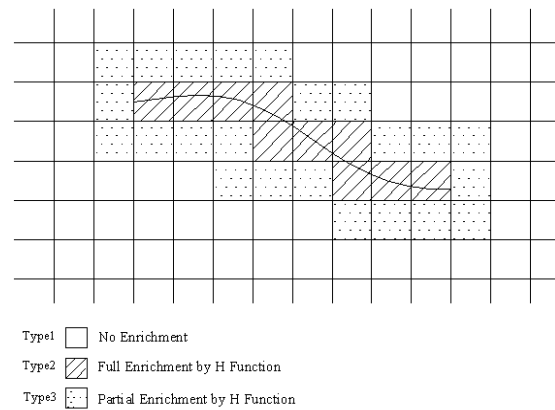


Fig. 3 Different areas of enrichment by the  $H$  function alone

## 2.3. XFEM formulation for Kirchhoff plate

The state of deformation of Kirchhoff plates can be presented by normal displacement  $w$  and the following fourth-order differential equation [18]:

$$D \left( \frac{\partial^4 w}{\partial x^4} + 2 \frac{\partial^4 w}{\partial x^2 \partial y^2} + \frac{\partial^4 w}{\partial y^4} \right) - p = 0, \quad (6)$$

in which  $p$  is the lateral load intensity and  $D$  (bending stiffness) is computed from:

$$D = \frac{E h^3}{12(1-\nu^2)}, \quad (7)$$

in the above,  $\nu$  is the Poisson's ratio,  $h$  is the plate thickness, and  $E$  is the Young's modulus. In this study we used 4-node rectangular elements for which each node has three degrees of freedom. Fig. 4 shows a typical element along with the related parameters. Accordingly, the discretized form of normal displacement  $w$  can be presented as:

$$w^h = \sum_{i=1}^I \sum_{l=1}^3 w_{il} N_{il}, \quad w_{il} = \begin{Bmatrix} w_i \\ \theta_{x_i} \\ \theta_{y_i} \end{Bmatrix}, \quad (8)$$

in which,  $I$  is the set of element nodes,  $w_i$  are the nodal values of normal displacement,  $\theta_{x_i}$  and  $\theta_{y_i}$  are the nodal values of rotation about  $x$  and  $y$  axis respectively, and  $N_{il}$  are the shape functions derived by Melosh [19].

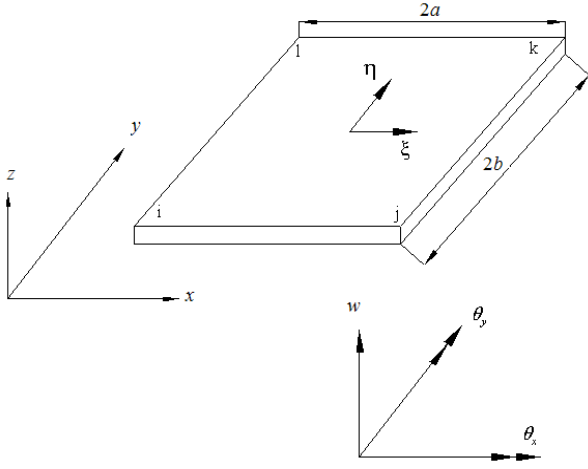


Fig. 4 A 4-node rectangular plate element in global and normalized coordinate systems

In dealing with cracked plates, we use the near crack tip stress and displacement fields for a crack in an infinite Kirchhoff plate provided by Williams [15], and the stress intensity factor definitions of Sih et al. [16] for the deflection fields to write:

$$w = \frac{(2r)^{3/2}(1-\nu^2)}{2Eh(3+\nu)} \left\{ K_1 \left[ \frac{1}{3} \left( \frac{7+\nu}{1-\nu} \right) \cos \frac{3\theta}{2} - \cos \frac{\theta}{2} \right] + K_2 \left[ -\frac{1}{3} \left( \frac{5+3\nu}{1-\nu} \right) \sin \frac{3\theta}{2} + \sin \frac{\theta}{2} \right] \right\}, \quad (9)$$

where  $K_1$  and  $K_2$  are symmetric (bending) and anti-symmetric (twisting) stress intensity factors. On the other hand, the enriched displacement approximation can be written as:

$$w^h = \sum_{i=1}^I \sum_{l=1}^3 N_{il}(x) w_{il} + \sum_{j=1}^J \sum_{l=1}^3 N_{jl}(x) H(x) d_{jl} + \sum_{k=1}^K \sum_{l=1}^3 N_{kl}(x) \left[ \sum_{m=1}^4 e_{kl}^m G_m(r, \theta) \right], \quad (10)$$

where  $I$ ,  $J$  and  $K$  are the sets defined in Eq. (5). The *Tip* functions  $G_m(r, \theta)$  can be extracted from the analytical solution by writing Eq. (9) in the following form:

$$w = C_1 r^{\frac{3}{2}} \sin\left(\frac{\theta}{2}\right) + C_2 r^{\frac{3}{2}} \cos\left(\frac{\theta}{2}\right) + C_3 r^{\frac{3}{2}} \sin\left(\frac{3\theta}{2}\right) + C_4 r^{\frac{3}{2}} \cos\left(\frac{3\theta}{2}\right), \quad (11)$$

where  $C_i$  are the constants which are independent of  $r$  and  $\theta$ . Since in the vicinity of crack tip the normal displacement  $w$  is a composition of these four expressions, the *Tip* functions can be chosen as:

$$\{G_l(r, \theta)\}_{l=1}^4 = \left\{ r^{\frac{3}{2}} \sin\left(\frac{\theta}{2}\right), r^{\frac{3}{2}} \cos\left(\frac{\theta}{2}\right), r^{\frac{3}{2}} \sin\left(\frac{3\theta}{2}\right), r^{\frac{3}{2}} \cos\left(\frac{3\theta}{2}\right) \right\}. \quad (12)$$

Note that the first and the third functions are discontinuous along the crack, which means that their values have a jump at the Gaussian points above and below the crack.

#### 2.4. Stress intensity factor (SIF) computation

In this study, the SIFs for the XFEM simulations were calculated using the J-Integral and the Interaction Integral methods. The basic formulations can be found in Appendix A. The results were compared with the following analytical solutions. The analytic solution for a finite-width plate with a central crack under remote tensile stress  $\sigma$  is [20]:

$$K_I = \sigma \sqrt{\pi a} \left[ \sec\left(\frac{\pi a}{2B}\right) \right]^{\frac{1}{2}} \times \left[ 1 - 0.025 \left(\frac{a}{B}\right)^2 + 0.06 \left(\frac{a}{B}\right)^4 \right], \quad (13)$$

in which,  $B$  is the plate width and  $a$  is half the crack length. The SIF expressions for an oblique through crack in an infinite plate under uni-axial loading are [20]:

$$\left. \begin{aligned} K_I &= \sigma \sqrt{\pi a} \cos^2(\beta); \\ K_{II} &= \sigma \sqrt{\pi a} \sin(\beta) \cos(\beta); \end{aligned} \right\} \quad (14)$$

where  $\beta$  is the angle between the normal to crack plane with the stress axis.

The SIF expressions for an infinite plate with a central through crack of the length  $2a$  under pure bending moment ( $M$ ) are [16]:

$$K_I = \frac{6M_0}{h^2} \sqrt{a}, \quad K_2 = 0. \quad (15)$$

### 3. Results and discussion

In this section some typical benchmark plane and plate problems are solved by the developed XFEM codes and the obtained result are compared with the existing analytic solutions.

As illustrated in Figs. 5, a and d, a usual practice in XFEM is to enrich the nodes of the crack tip element by the *Tip* functions and the nodes of the crack wake elements by the  $H$  function. However, if only the  $H$  function is used for enrichment, two different schemes can be proposed for the enrichment of the tip element nodes. In the first scheme (H1 scheme), all the nodes are enriched by the  $H$  function (Figs. 5, b and e). In the second scheme (H2 scheme) the nodes of the front edge are excluded from the enrichment (Figs. 5, c and f).

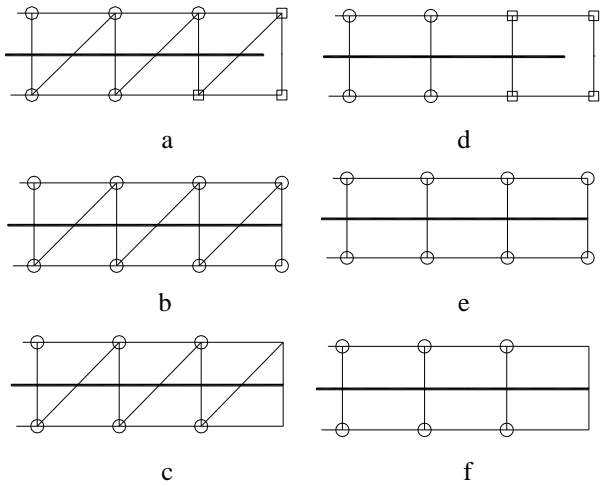


Fig. 5 Different enrichment schemes used for CST and Q4 elements. The nodes enriched by the *Tip* and *H* functions are shown by quadrangles and circles respectively. a) HT Scheme for CST; b) H1 Scheme for CST; c) H2 Scheme for CST; d) HT Scheme for Q4; e) H1 Scheme for Q4; f) H2 Scheme for Q4

3.1. Rectangular plate with a straight through crack under remote tension

Fig. 6 shows a rectangular plate containing a through-thickness crack under uniform tension. This problem is solved using CST and Q4 elements according to the

prescribed schemes and the results are compared with analytical solutions.

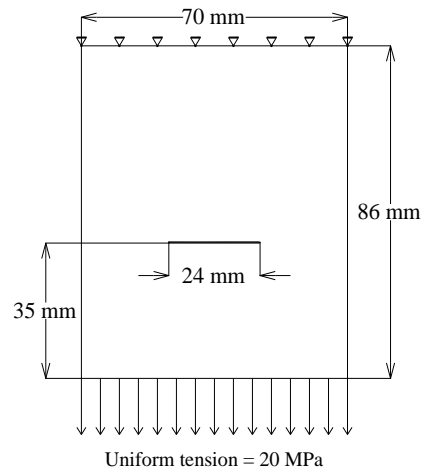


Fig. 6 A rectangular plate with a straight crack under uniform tension

The normalized stress intensity factor values for different number of elements are listed in Tables 1 and 2. It is clear that the results of both HT and H2 schemes are in excellent agreement with the analytical solution, while the results of the H1 scheme are slightly higher. Although both the Interaction Integral and the J-Integral methods are efficient in evaluating SIFs, the results of the former method agree better with the analytical values.

Table 1

Normalized analytic and numeric SIF values for a rectangular plate with a straight through crack under remote tension (CST- XFEM code)

SIF	Analytical solution	No. of elements in mesh	Interaction Integral			J-Integral		
			HT Scheme	H1 Scheme	H2 Scheme	HT Scheme	H1 Scheme	H2 Scheme
$\frac{K_I}{\sigma\sqrt{\pi a}}$	1.075	3000	1.076	1.100	1.042	1.067	1.137	0.993
		4000	1.088	1.127	1.068	1.081	1.162	1.046
		6000	1.092	1.136	1.075	1.096	1.179	1.060

Table 2

Normalized analytic and numeric SIF values for a rectangular plate with a straight through crack under remote tension (Q4- XFEM code)

SIF	Analytical solution	No. of elements in mesh	Interaction Integral			J-Integral		
			HT Scheme	H1 Scheme	H2 Scheme	HT Scheme	H1 Scheme	H2 Scheme
$\frac{K_I}{\sigma\sqrt{\pi a}}$	1.075	1500	1.100	1.140	1.079	1.104	1.029	0.957
		2000	1.095	1.136	1.083	1.104	1.029	0.967
		3000	1.094	1.127	1.084	1.103	1.052	1.002

3.2 Rectangular plate with an oblique through crack under remote tension

Fig. 7 shows a rectangular plate containing an oblique through-thickness crack under uniform tension. The stress intensity factors for Modes I and II are evaluated by Eq. (14) and the CST-XFEM code using different enrichment schemes. It should be noted that although

Eq. (14) presents the same values for both crack tips and does not consider the effects of finite sizes, in practice the SIFs for the two crack tips are different and their values for a finite width plate are higher than those for an infinite plate. The normalized stress intensity factor values obtained by the Interaction Integral and the J-Integral methods are listed in Tables 3 and 4 respectively.

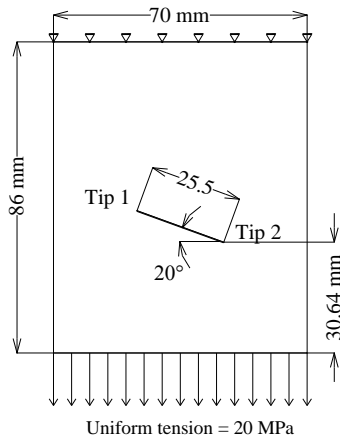


Fig. 7 A rectangular plate with an oblique crack under uniform tension

It is clear that the results of HT and H2 schemes are in better agreement with the analytic results and the J-Integral results are lower than the Interaction Integral results. Considering the effects of finite width on Eq. (14), it seems that the results of the Interaction Integral method are more precise than the J-Integral method. Moreover, we found noticeable variations of the KI and KII values on different contours using the J-Integral method. Thus, the SIFs listed in Table 4 are the average values. Although the Interaction Integral values on different contours were not exactly the same, the variation was quite limited and a specific value could be considered for a range of contours.

Table 3

Normalized analytic and numeric SIF values for a rectangular plate with an oblique through crack under remote tension using the Interaction Integral method. (CST- XFEM code)

SIFs.	Analytical solution	No. of elements in mesh	HT Scheme		H1 Scheme		H2 Scheme	
			Tip1	Tip2	Tip1	Tip2	Tip1	Tip2
$\frac{K_I}{\sigma\sqrt{\pi a}}$	0.883	3000	0.917	0.931	0.935	0.953	0.900	0.915
		4000	0.914	0.933	0.940	0.953	0.905	0.924
		6000	0.914	0.930	0.946	0.969	0.905	0.924
$\frac{K_{II}}{\sigma\sqrt{\pi a}}$	0.321	3000	0.440	0.410	0.462	0.433	0.430	0.408
		4000	0.438	0.411	0.452	0.430	0.440	0.407
		6000	0.436	0.408	0.455	0.424	0.432	0.414

Table 4

Normalized analytic and numeric SIF values for a rectangular plate with an oblique through crack under remote tension using the J-Integral method. (CST- XFEM code)

SIFs.	Analytical solution	No. of elements in mesh	HT Scheme		H1 Scheme		H2 Scheme	
			Tip1	Tip2	Tip1	Tip2	Tip1	Tip2
$\frac{K_I}{\sigma\sqrt{\pi a}}$	0.883	3000	0.848	0.881	0.901	0.976	0.805	0.828
		4000	0.861	0.879	0.898	0.968	0.821	0.849
		6000	0.844	0.872	0.937	0.980	0.820	0.851
$\frac{K_{II}}{\sigma\sqrt{\pi a}}$	0.321	3000	0.495	0.462	0.515	0.464	0.489	0.458
		4000	0.491	0.463	0.518	0.464	0.504	0.422
		6000	0.509	0.466	0.516	0.474	0.500	0.458

3.3. Rectangular plate with a through crack under pure bending

Fig. 8 illustrates a pure bending problem with the stress intensity factors expressed by Eq. (15).

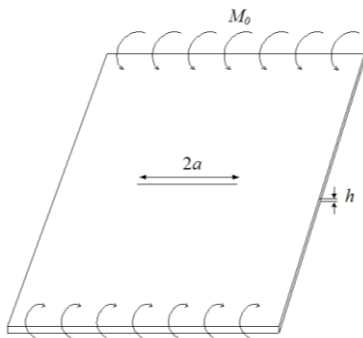


Fig. 8 A rectangular plate with through crack under pure bending

This benchmark problem is simulated with a finite length rectangular plate. The plate dimensions are 86×70 mm and  $h = 1$  mm, the applied moment ( $M_0$ ) is 10 Nmm/mm, and the problem is solved for different crack lengths.

The SIFs are computed based on the integrals obtained for circular domains with different radii (ranging from a quarter length of crack to half length of crack) and the average values are listed in Table 5. Although  $K_I$  values for different contours were not exactly the same, the difference between minimum and maximum values did not exceed 10% of the mean value. It is clear that the best results are obtained with the HT scheme and the H1 and H2 scheme provide higher and lower values with respect to the analytical results respectively.

Symmetric bending SIF and its normalized values for rectangular plate with through crack under pure bending

Crack Length, mm	Eq. (15), MPa√mm	HT Scheme, MPa√mm	$\frac{K_I \text{ (HT Scheme)}}{K_I \text{ (Eq. (15))}}$	H1 Scheme, MPa√mm	$\frac{K_I \text{ (H1 Scheme)}}{K_I \text{ (Eq. (15))}}$	H2 Scheme, MPa√mm	$\frac{K_I \text{ (H2 Scheme)}}{K_I \text{ (Eq. (15))}}$
12	146.97	143	0.973	156	1.061	136.5	0.929
16	169.71	165.5	0.975	181	1.067	158.5	0.934
20	189.74	186	0.98	204	1.075	180.5	0.951
24	207.85	206	0.991	226	1.087	198	0.953
28	224.5	223	0.993	245	1.091	216	0.962

#### 4. Conclusion

Although the implementation of *Tip* functions in the node enrichment procedure around crack tip is a usual practice in XFEM, it naturally involves creation of abnormal elements and also leads to additional complications in the basic FEM formulation. In this study we compared the sole usage of the H function with a combined usage of both the H and the *Tip* functions in the enrichment process. It was shown that for the proposed enrichment schemes the elimination of the *Tip* functions has no noticeable effect on the accuracy of the computed stress intensity factors for the plane problems. It was also shown that for both CST and Q4 elements, the performance of the H2 scheme (with limited enrichment) was better than the H1 scheme.

We also studied the XFEM modelling of cracked plates under out of plane bending using the new *Tip* functions extracted from analytical solutions of Kirchhoff plates. It was found that, in contrast to the plane problems, the combined usage of the H and *Tip* functions in the enrichment procedure (HT Scheme) provided excellent results, while the results of H1 and H2 schemes were less satisfactory.

The performance of the J-Integral and the Interaction Integral methods in evaluating the stress intensity factors for plane XFEM problems was also studied. Although both methods provided very accurate results, the Interaction Integral results were in general more precise. Moreover, while the Interaction Integral values remained stable along different computation contours, in some cases the J-Integral showed unfavourable fluctuations with changing the contour radius.

#### Appendix A

The J-Integral method is widely used for numerical determination of SIFs. For a plane problem, this contour integral is defined by:

$$J = \int_{\Gamma} \left( W dy - T_i \frac{\partial u_i}{\partial x} ds \right), \quad (A1)$$

in which  $T_i$  and  $u_i$  are defined on the contour  $\Gamma$  (as the traction and displacement components respectively), and  $W$  is the strain energy density inside the contour.

Numerical computation of the above contour integral is rather difficult, so it is usually changed into a domain form:

$$J = \int_A \left[ \left( \sigma_{ij} \frac{\partial u_i}{\partial x_j} - W \delta_{ij} \right) \frac{\partial q}{\partial x_i} \right] dA, \quad (A2)$$

where  $q$  is a sufficiently smooth weighting function which takes a value of unity on an open set containing the crack tip and vanishes on an outer prescribed contour.

In the mixed mode conditions, Eqs. (A1) and (A2) do not allow  $K_I$  and  $K_{II}$  to be calculated separately. In this case, invariant integrals can be used as below [21]:

$$J_k = - \int_A \left( W \frac{\partial q}{\partial x_k} - \sigma_{ij} \frac{\partial u_i}{\partial x_k} \frac{\partial q}{\partial x_j} \right) dA - \int_A \left\{ \frac{\partial W}{\partial x_k} - \sigma_{ij} \frac{\partial}{\partial x_j} \left( \frac{\partial u_i}{\partial x_k} \right) \right\} q dA - \int_C t_i \frac{\partial u_i}{\partial x_k} q ds, \quad (A3)$$

where  $k$  is an index for local crack tip axis ( $x, y$ ). The stress intensity factors can be obtained from above integrals by the following relationships:

$$\left. \begin{aligned} K_I &= 0.5 \sqrt{\frac{8\mu}{\kappa+1}} \left( \sqrt{J_1 - J_2} + \sqrt{J_1 + J_2} \right) \\ K_{II} &= 0.5 \sqrt{\frac{8\mu}{\kappa+1}} \left( \sqrt{J_1 - J_2} - \sqrt{J_1 + J_2} \right) \end{aligned} \right\}. \quad (A4)$$

Another efficient method for numerical computation of SIF (especially in mixed mode problems) is the Interaction Integral method [4]. In this method two states of a cracked body are considered. The state1 ( $\sigma_{ij}^{(1)}, \varepsilon_{ij}^{(1)}, u_i^{(1)}$ ) corresponds to the present state and the state2 ( $\sigma_{ij}^{(2)}, \varepsilon_{ij}^{(2)}, u_i^{(2)}$ ) is an auxiliary state which will be chosen as the asymptotic fields for Mode I or Mode II. For a plane problem, the Interaction Integral is defined as:

$$I^{(1,2)} = \int_A \left[ \sigma_{ij}^{(1)} \frac{\partial u_i^{(2)}}{\partial x_j} + \sigma_{ij}^{(2)} \frac{\partial u_i^{(1)}}{\partial x_j} - W^{(1,2)} \delta_{ij} \right] \frac{\partial q}{\partial x_j} dA, \quad (A5)$$

where  $W^{(1,2)}$  is the interaction strain energy:

$$W^{(1,2)} = \sigma_{ij}^{(1)} \varepsilon_{ij}^{(2)} = \sigma_{ij}^{(2)} \varepsilon_{ij}^{(1)}. \quad (A6)$$

The relationship between the Interaction Integral and SIF is:

$$I^{(1,2)} = \frac{2}{E^*} \left( K_I^{(1)} K_I^{(2)} + K_{II}^{(1)} K_{II}^{(2)} \right) \quad (A7)$$

where  $E^*$  is defined in terms of  $E$  (Young's modulus) and  $\nu$  (poisson's ratio) as:

$$E^* = \begin{cases} E \rightarrow \text{plain\_stress}; \\ \frac{E}{1-\nu^2} \rightarrow \text{plain\_strain}. \end{cases} \quad (\text{A8})$$

Making a judicious choice of state 2 as the pure Mode I asymptotic field with  $K_I^{(2)} = 1$ ,  $K_{II}^{(2)} = 0$  gives the Mode I stress intensity factor for state 1 in terms of the Interaction Integral:

$$K_I^{(1)} = \frac{2}{E^*} I^{(1, \text{Mode I})}. \quad (\text{A9})$$

The Mode II stress intensity factor can be determined in a similar fashion

Similarly, for plate bending problems, the J-Integral is defined as:

$$J_k = \oint_{\Gamma} \left\{ W \delta_{k,\beta} - [M_{\alpha\beta} \theta_{\alpha,k} + Q_{\beta} w_{,k}] \right\} n_{\beta} d\Gamma, \quad (\text{A10})$$

where  $\alpha, \beta = 1, 2$  and  $M_{\alpha\beta}$  and  $Q_{\beta}$  are the moment and the shear force components and  $W$  is the strain energy density defined as:

$$W = \frac{1}{2} [M_{\alpha\beta} \theta_{\alpha,\beta}]. \quad (\text{A11})$$

Choosing  $k = 1$  in (A11), the first mode (bending mode) can be written as:

$$J_1 = \oint_{\Gamma} \left\{ W \delta_{1,\beta} - [M_{\alpha\beta} \theta_{\alpha,1} + Q_{\beta} w_{,1}] \right\} n_{\beta} d\Gamma. \quad (\text{A12})$$

Using the divergence theory, this integral can be converted to a domain integral which is convenient for numerical computations. The relationship between the SIF and the J-Integral is [22]:

$$J_1 = \frac{\pi}{3E} \left( \frac{1+\nu}{3+\nu} \right) (K_I^2) \Rightarrow K_I = \sqrt{\left( \frac{3+\nu}{1+\nu} \right) \frac{3E}{\pi} J_1}. \quad (\text{A13})$$

## References

1. **Jakušovas, A.; Daunys, M.** 2009. Investigation of low cycle fatigue crack opening by finite element method, *Mechanika* 3(77): 13-17.
2. **Shariati, M.; Sedighi, M.; Saemi, J.; Eipakchi, H.R.; Allahbakhsh, H.R.** 2010. Numerical and experimental investigation on ultimate strength of cracked cylindrical shells subjected to combined loading, *Mechanika* 4(84): 12-19.
3. **Belytschko, T.; Black, T.** 1998. Elastic crack growth in finite elements with minimal remeshing, *International Journal for Numerical Methods in Engineering* 45(5): 601-620. <http://dx.doi.org/10.1002/nme.598>.
4. **Dolbow, J.** 1999. An extended finite element with discontinuous enrichment, PhD thesis, Northwestern University.
5. **Sukumar, N.; Moës, N.; Moran, B.; Belytschko, T.** 2000. Extended finite element method for three-dimensional crack modelling, *International Journal for Numerical Methods in Engineering* 48(11): 1549-1570. <http://dx.doi.org/10.1002/nme.955>.
6. **Belytschko, T.; Chen, H.; Xu, J.; Zi, G.** 2003. Dynamic crack propagation based on loss of hyperbolicity and a new discontinuous enrichment, *International Journal for Numerical Methods in Engineering* 58(12): 1873-1905. <http://dx.doi.org/10.1002/nme.941>.
7. **Moës, N.; Belytschko, T.** 2002. Extended finite element method for cohesive crack growth, *Engineering Fracture Mechanics* 69(7): 813-833. [http://dx.doi.org/10.1016/S0013-7944\(01\)00128-X](http://dx.doi.org/10.1016/S0013-7944(01)00128-X).
8. **Dolbow, J.; Gosz, M.** 2002. On the computation of mixed-mode stress intensity factors in functionally graded materials, *International Journal of Solids and Structures* 39(9): 2557-2574. [http://dx.doi.org/10.1016/S0020-7683\(02\)00114-2](http://dx.doi.org/10.1016/S0020-7683(02)00114-2).
9. **Asadpoure, A.; Mohammadi, S.; Vafai, A.** 2006. Crack analysis in orthotropic media using the extended finite element method, *Thin-Walled Structures* 44(9): 1031-1038. <http://dx.doi.org/10.1016/j.tws.2006.07.007>.
10. **Abdelaziz, Y.; Nabbou, A.; Hamouine, A.** 2009. A state-of-the-art review of the X-FEM for computational fracture mechanics, *Applied Mathematical Modelling* 33(12): 4269-4282. <http://dx.doi.org/10.1016/j.apm.2009.02.010>.
11. **Dolbow, J.; Moës, N.; Belytschko, T.** 2000. Modeling fracture in Mindlin-Reissner plates with the extended finite element method, *International Journal of Solids and Structures* 37(48-50): 7161-7183. [http://dx.doi.org/10.1016/S0020-7683\(00\)00194-3](http://dx.doi.org/10.1016/S0020-7683(00)00194-3).
12. **Areias, P.M.A.; Belytschko, T.** 2005. Non-linear analysis of shells with arbitrary evolving cracks using XFEM, *International Journal of Numerical Methods in Engineering* 62(3): 384-415. <http://dx.doi.org/10.1002/nme.1192>.
13. **Areias, P.M.A.; Song, J.H.; Belytschko, T.** 2006. Analysis of fracture in thin shells by overlapping paired elements, *Computer Methods in Applied Mechanics and Engineering* 195(41-43): 5343-5360. <http://dx.doi.org/10.1016/j.cma.2005.10.024>.
14. **Kirchhoff, G.** 1850. Über das Gleichgewicht und die Bewegung einer elastischen Scheibe, *J. für Reine und angewandte Mathematik* 1859(40): 51-88. <http://dx.doi.org/10.1515/crll.1850.40.51>.
15. **Williams, M.** 1961. The bending stress distribution at the base of a stationary crack, *Journal of Applied Mechanics* 28: 78-82.
16. **Sih, G.; Paris, P.; Erdogan, F.** 1962. Crack-tip stress-intensity factors for plane extension and plate bending problems, *Journal of Applied Mechanics* 29: 306-312. <http://dx.doi.org/10.1115/1.3640546>.
17. **Chessa, J.** 2003. The extended finite element method for free surface and two phase flow problems, PhD thesis, Northwestern University.
18. **Zienkiewicz, O.C.; Taylor, R.L.** 2000. The Finite Element Method volume 2: The Basis, Butterworth Heinemann.
19. **Melosh, R.J.** 1963. Structural analysis of solids, *ASCE Structural Journal* 89(4): 205-223.
20. **Anderson, T.L.** 1995. *Fracture Mechanism Fundamentals and Applications*. Boca Raton, Ana Arbor: CRC

Press. 793p.

21. **Araújo, T.D.; Bittencourt, T.N.; Roehl, D.; Martha, L.F.** 2000. Numerical estimation of fracture parameters in elastic and elastic-plastic analysis, In: "European Congress on Computational Methods in Applied Sciences and Engineering", Barcelona, pp. 11-14.
22. **Hui, C. Y.; Zehnder, A.** 1993. A theory for the fracture of thin plates subjected to bending and twisting moments, *International Journal of Fracture* 61: 211-229.

S.J. Rouzegar, M. Mirzaei

## 2D PLYŠIO MODELIAVIMAS IŠPLĖSTINIŲ BAIGTINIŲ ELEMENTŲ METODU

### R e z i ū m ė

Šiame darbe 2D plyšiui modeliuoti plokštumose ir plokštelėse buvo taikomas išplėstinis baigtinių elementų metodas (IBEM). Buvo siekiama ištirti svertinių plyšio funkcijų svarbą mazgais praturtintoje procedūroje. Iš Kirchhofo plokštelių analitinių sprendinių buvo išrinktas naujas svertinių funkcijų tinklėlis ir išanalizuotos įvairios mazginės plokštumų ir plokštelių pagerinimo schemas. Įtempių intensyvumo koeficientai (IIV) tipiniams etaloniškiems uždaviniams spręsti buvo apskaičiuoti J integralų ir sąveikos integralų metodais. Rezultatai rodo, kad svertinių funkcijų panaikinimas neturėjo didelio poveikio įtempių intensyvumo koeficientų plokštumos uždaviniuose tikslumui. Tačiau apskaičiuotų plokštelių reikšmių tikslumas šios procedūros buvo gana stipriai veikiamas. Be to, buvo nustatyta, kad sąveikos integralo metodas geriau tiko plyšio parametrų skaičiavimui.

S. J. Rouzegar, M. Mirzaei

## A COMPARATIVE STUDY ON 2D CRACK MODELLING USING EXTENDED FINITE ELEMENT METHOD

### S u m m a r y

In this study the Extended Finite Element Method (XFEM) was used for modelling 2D cracks in plane and plate problems. The aim was to investigate the significance of the crack *Tip* functions in the nodal enrichment procedure. A new set of *Tip* functions were extracted from analytical solutions of Kirchhoff plates and various nodal enrichment schemes were examined for plane and plate elements. The stress intensity factors (SIF) for typical benchmark problems were calculated using the J-Integral and the Interaction Integral methods. The results indicated that elimination of the *Tip* functions had no noticeable effect on the accuracy of the computed stress intensity factors for the plane problems. However, the precision of the computed values for the plate problems were quite affected by this procedure. Moreover, the Interaction Integral method was found to be more efficient for the computation of crack parameters in such problems.

**Keywords:** Extended finite element, Nodal enrichment, Interaction Integral, J-Integral fracture.

Received February 08, 2012

Accepted June 17, 2013